

AGN variability: from Seyfert nuclei to QSOs

Itziar Aretxaga¹

RESUMEN

Las propiedades del continuo óptico de los Núcleos Galácticos Activos son revisadas, encontrándose que las variaciones producidas en objetos débilmente radioemisores son consistentes con aquellas esperadas en modelos Poissonianos, en los que la luminosidad es el producto de la superposición de pulsos individuales. En este contexto se describen las predicciones del modelo de Formación Estelar Violenta.

ABSTRACT

The continuum variability of optically selected Active Galactic Nuclei (AGN) is found to be consistent with that expected from a simple Poissonian process, in which the total luminosity of an object is produced by the multiple superposition of identical pulses. The energies, time-scales and rates of the pulses are found to be in the range of those expected from supernovae which generate fast evolving remnants in a nuclear starburst. However, radio-loud AGN don't follow the predictions of that simple scenario.

1. INTRODUCTION

Variability is a common characteristic of AGN. Even among brands which classically have been regarded as quiescent, LINERs and Seyfert 2 nuclei, there are reported cases of variations in both lines and continuum — see for example the development of broad lines and increase of continuum luminosity in the LINER NGC 1097 (Storchi-Bergmann et al. 1993) or in the Seyfert 2 nucleus Mrk 993 (Tran et al. 1992). Classically variable brands are Seyfert 1 nuclei and QSOs, with simultaneous time-scales of variation which range from a few years to a few weeks (see the sketch in Smith et al. 1991) and involve integrated B -band energies of up to several times 10^{50} erg. In some of these radio-quiet AGN intra-day variability has also been found (Dultzin-Haczan et al. 1992, Gopal-Krishna et al. 1995), a mode which is common in blazar-type objects (Wagner et al. 1990).

Continuum variability is a popular tool to assess models of AGN and, although detailed predictions are rarely available, there is considerable debate about trends in the variability relationships which can rule out or backup one model or another.

2. QSO VARIABILITY FROM ENSEMBLE LIGHT CURVES

Much of our knowledge about QSO variability is based on studies of large samples of sources monitored on photographic plates over a period of one or two decades. Although each individual QSO is poorly monitored in these samples (typically 10–20 epochs), the rationale is that the ensemble light curve of all QSOs will give general information about the individuals. In the last decade several studies have shown that variability is anti-correlated with luminosity, in the sense that luminous QSOs have smaller amplitude variations than low-luminosity ones (e.g. Pica & Smith 1983, Hook et al. 1994). The anti-correlation is somewhat flatter than a “ $1/\sqrt{N}$ ” law, a result which seems to rule out simple Poissonian models, in which the variations are created by a random superposition of identical events, or pulses.

2.1. Danger in wavelength effects

However, these studies disregard the fact that AGN variability is wavelength dependent. It is known that in nearby AGN the amplitude of variations increases towards shorter wavelengths. This is illustrated in Kinney et al. (1991) where the continuum variations across the UV spectrum are shown for all the AGN in the IUE database. A quantitative study of the Seyfert 1 nuclei and QSOs ($z < 1.3$) in this sample states that in

¹Royal Greenwich Obs. Madingley Rd. Cambridge, CB3 0EZ, UK

the $\lambda 1200\text{--}3200 \text{ \AA}$ range the rms of the luminosity changes by about $(6.2 \pm 4.3)\%$ every 1000 \AA (Paltani & Courvoisier 1994). Indirect evidence that wavelength effects are also present in high-redshift QSOs was derived from parametric fits to single pass-band variability data (Cristiani et al. 1996, Cid Fernandes, Aretxaga & Terlevich 1996, hereafter CAT96); but the first direct evidence for this effect has been presented by Cristiani et al. in this conference, showing that the R -band amplitude of variability in a sample of 149 QSOs is smaller by a factor 1.13 ± 0.05 than in B -band.

The variability measured at a fixed optical band tends to overestimate the monochromatic rest frame optical variability, simply because the objects at higher redshifts are observed at bluer emitted wavelengths. Wavelength effects must be removed before analyzing the variability dependence with luminosity and deriving implications for Poissonian models. Indeed, parametric fits to the variability–luminosity–redshift space (CAT96) show that if QSOs in general follow a wavelength–variability relationship similar to that of nearby AGN ($\sigma \propto \lambda^{-b}$, with $0.5 < b < 1.5$, where σ is the rms of the luminosity), then the variability–luminosity relationship $\sigma \propto L^{-a}$ can be bracketed to values $-0.8 < a < -0.3$ and, therefore, is consistent with a simple Poissonian model ($a = -0.5$).

2.2. Parameters for a simple Poissonian model

The variability generated by a Poissonian process is characterized by the following parameters:

1. the percentage of a non-variable “background” component, if it exists (f_{bck});
2. the time-scale of the events (τ);
3. the energy of the events (ϵ);
4. the rate of events (ν).

An upper limit for the background fraction of light can be directly estimated from the minima of the light curves of QSOs: $f_{bck} \lesssim L_{min}/\overline{L}$. This fraction is $f_{bck} < 0.7$ for the SGP sample, 283 QSOs at $0.43 < z < 4.01$ observed in B -band for 7 epochs in a time span of 16 yr (Hook et al. 1994).

The time-scale of the pulses can be derived from the ensemble Structure Function (SF) of QSOs. The SF is the curve of growth of variability with time, formally defined as $SF(\Delta t) = \langle m_i - m_j \rangle$, where i and j are all the possible epochs which satisfy that $|t_i - t_j| \approx \Delta t$, and m are the magnitudes of any QSO in the database at those epochs. Hook et al. (1994) and Cristiani et al. (1996) showed that the ensemble SF rises steadily for $\Delta t \lesssim 2 - 3$ yr and flattens at larger lags. Therefore we can regard the pulse life-time to be $1.5 \lesssim \tau \lesssim 3$ yr.

The energy of the pulses can be estimated from fits of the form $\sigma \propto L^a(1+z)^b$ to the data (CAT96). Note that the redshift term is analogous to the wavelength term discussed in section 2.1. The proportionality constant of the $\sigma - L - z$ relationship is directly linked to the background fraction and to the luminosity of each pulse. Since the energy and the luminosity of the pulses are related by the pulse life-time, the energy ϵ is found to be $1.5 \times 10^{50} \lesssim \epsilon \lesssim 6.3 \times 10^{51}$ erg, within the limits of f_{bck} and τ given in this section.

From the total variable luminosity of the QSOs $(1 - f_{bck})\overline{L}$ and the energy of the pulses, we derive that the rate of events is $3 \lesssim \nu \lesssim 150 \text{ yr}^{-1}$ for a $M_B = -25$ mag QSO, within the limits of f_{bck} , τ and ϵ given above.

Although the range of parameters is not tightly constrained, it gives us an idea of the parameter-space to look for event candidates.

3. SEARCH OF ‘PULSES’ IN SEYFERT NUCLEI

Any search of isolated pulses of variation will be more satisfactorily carried out in Seyfert 1 nuclei than in QSOs. Seyfert nuclei share all the properties of QSOs across the electromagnetic spectrum, and are generally regarded as lower luminosity counterparts of QSO activity in the nearby Universe. It is their lower luminosity ($M_V > -23$ mag) which makes them attractive for attempts to isolate pulses of variation, since the rate of events in these objects is predicted to be so much lower.

In their study of the historical optical light curve of NGC 4151 ($\overline{M_B} \sim -20$ mag) Aretxaga & Terlevich (1994a, hereafter AT94) draw the attention to a sharp pulse which raised from a deep minimum in 1970 and lasted for a few weeks, followed by a second peak of slow decline (a few years) with at least two secondary maxima — see fig.1. The second peak comprises a B -band energy of $\epsilon \approx 3 \times 10^{50}$ erg. They found some other similar events in the light curve of NGC 4151, reaching the conclusion that the pattern of the light curve could be originated by the superposition of a basic unit of variation, isolated in the 1970–1973 event.

Perhaps the most impressive repetition of this kind of double-peak event has been found in NGC 5548 ($\overline{M_B} \sim -21.1$ mag), tightly monitored by the AGN Watch consortium since late 1988 (Korista et al. 1995 and

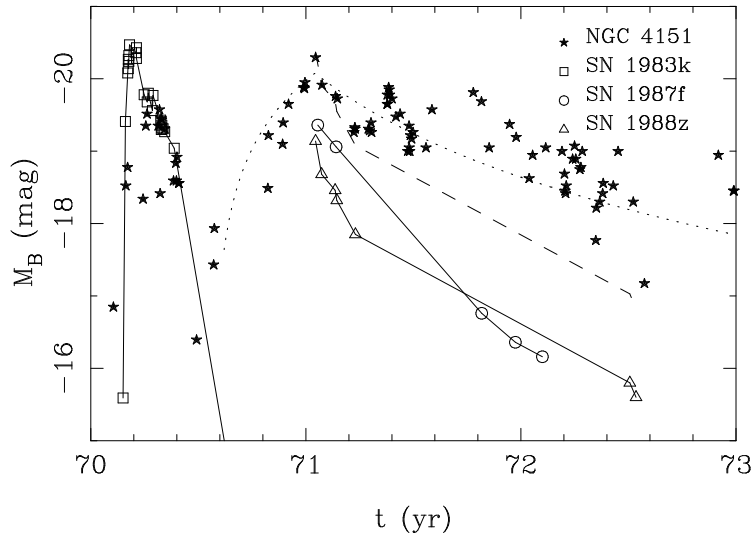


Fig. 1. Comparison of the net variation of the B -band light curves of NGC 4151 and SN 1983K, SN 1987F and SN 1988Z. The dotted line shows the theoretical B -band light curve of a cSNR ($\epsilon_{51} = 3$, $n_7 = 1$). The dashed line represents the light curve of SN 1988Z, scaled to match the second peak of the light curve of NGC 4151.

references therein). After a deep minimum in 1992 when the nucleus lost almost all its broad $H\beta$ line (Iijima et al. 1992), the light curve developed a double-peak event as that of NGC 4151, with secondary maxima in the second slow-decay peak at similar time-scales as those of NGC 4151, and similar energies (Cid-Fernandes, Terlevich & Aretxaga 1996). As in NGC 4151, previous events in the light curve were identified to approximately match the pattern of the double-peak event.

NGC 4151 and NGC 5548 are by far the historically best followed up Seyfert nuclei. But even in the much scarcely monitored low-luminosity ($\overline{M}_B \gtrsim -18$ mag) NGC 1516 the double-peak pattern can be detected (see Alloin et al. 1986) where, however, the time-scale of the slow-decay peak seems to be larger.

4. THE STARBURST MODEL: A PHYSICAL POISSONIAN MODEL

The conventional wisdom is that AGN variability is produced by instabilities in the accretion disk around a supermassive black hole (e.g. Rees 1984, Wallinder et al. 1992). However, to date there are no specific predictions in this model for the behaviour of the optical continuum. An important question in this respect is whether such instabilities should produce well defined patterns in the light curves, or whether the number of events should be correlated with the intrinsic luminosity of the object, as discussed in the previous sections.

The starburst model, reviewed by Cid Fernandes in this volume, gives a natural explanation for those effects. In this context, the optical variability observed in AGN is produced by supernovae (SNe) which generate rapidly evolving compact supernova remnants (cSNRs) due to the interaction of their ejecta with the high density circumstellar environment created by their progenitor stars. During the SN II phase, when the stellar cluster is 10–60 Myr old, the bolometric luminosity is dominated by stars, while the basic broad line region properties can be ascribed to the evolution of cSNRs in a medium with densities $n \gtrsim 10^7 \text{ cm}^{-3}$ (Terlevich et al. 1992). The observational evidence that most strongly supports this picture is the striking similarities of the optical spectra and light evolution of AGN and cSNRs, like SN 1987F or SN 1988Z, the so-called ‘Seyfert 1 impostors’ (Filippenko 1989).

4.1. The basic unit of variation

The two main features of the light curve in fig.1, the rapid first peak (70.2) and the second slower-decay peak (71) with secondary maxima, were compared with published light curves of SNe (AT94), finding that the 70.2 peak was reproduced in luminosity and shape by classical type II SNe, like SN 1983K. The 71 peak had the

same decline rate as cSNRs like SN 1987F and SN1988Z. Although these objects seem to be less luminous than NGC 4151, they are believed to have a high intrinsic extinction since they are embedded in H II regions. While there is no observational confirmation of cSNRs developing secondary maxima in their light curves (the wiggles in NGC 4151 after 71), hydro-dynamical models of cSNRs show that the bolometric luminosity undergoes secondary peaks of about 10^{49} – 10^{50} erg associated with thin shell formation and shell-shell collision, as well as time-unresolved rapid variability associated with cooling instabilities (Plewa 1995).

Therefore, *the basic unit of variation represented in fig.1 is associated with the explosion of a SN (70.2 peak) which develops a cSNR (71 peak)*. A simple semi-analytical approximation of the light curve of a cSNR is given by $L_B = 6 \times 10^9 L_B^\odot \epsilon_{51}^{7/8} n_7^{3/4} (t/t_{sg})^{-11/7}$ for $t > t_{sg}$, where $t_{sg} = 0.62 \text{ yr } \epsilon_{51}^{1/8} n_7^{-3/4}$ is the cooling time, ϵ_{51} is the bolometric energy released in each remnant in units of 10^{51} erg, and n_7 is the circumstellar density in which the cSNR evolves, in units of 10^7 cm^{-3} (Terlevich et al. 1992). This light curve for $\epsilon_{51} = 3$ and $n_7 = 1$ is represented in fig. 1 with a dotted line.

4.2. Intrinsic scaling relationships

The B-band luminosity arising from a coeval stellar cluster at its SN II explosion phase is mainly due to the contribution of main sequence stars and SNe. The SN rate (ν_{SN}) and the optical luminosity coming from stars (L_B^*) are related along the lifetime of this phase by $\nu_{SN}/L_B^* \approx 2 \times 10^{-11} \text{ yr}^{-1} L_B^\odot^{-1}$, almost independently of the IMF and age of the cluster (AT94). From this, we deduce that the mean total luminosity of the cluster is related to the SN rate by

$$\overline{L_B^{clu}} \sim 5 \times 10^{10} \frac{\nu_{SN}}{\text{yr}^{-1}} (\epsilon_B + 1) L_B^\odot, \quad (1)$$

where ϵ_B is the mean B-band energy released in each SN remnant, in units of 10^{51} erg. An estimation of ϵ_B can be obtained from the observed time-averaged equivalent width of H β ,

$$\overline{W_{H\beta}} \sim 320 \text{ \AA} \frac{\epsilon_B}{1 + 0.17\epsilon_B}, \quad (2)$$

which is also independent of the age, mass or IMF of the cluster, but is weakly dependent on the adopted bolometric correction of cSNRs (AT94). For SN 1987F and SN 1988Z we find $\epsilon_B/\epsilon_{51} \approx 0.12$. The near-constancy of the time-averaged equivalent width of H β is a central result of the starburst model. If the energy per supernova has a universal value, then the equivalent width of H β in AGN with broad lines should be in a narrow range of values.

4.3. Parameters of the model

From these expressions we can deduce that *the four parameters that characterize a Poissonian process can be described with just one functional parameter in the starburst model* (Aretxaga, Cid Fernandes & Terlevich 1996, ACT96 hereafter):

1. The main source of non-variable background luminosity comes from the stars in the cluster. The stellar luminosity is directly linked to the rate of events by a universal value. This makes for approximately half of the total luminosity of the nucleus.
2. The energy of the events is $\epsilon_B \sim 5 \times 10^{50}$ erg, in order to satisfy eq.2 with the observed values of the equivalent width of H β in QSOs, $\overline{W_{H\beta}} \approx 100 \text{ \AA}$ (Osterbrock 1991). Values of the kinetic energy released in a SN explosion of up to 3×10^{51} erg are measured in type II SNe (Branch et al. 1981).
3. The rate of events is linked to the total luminosity of the objects by eq.1, and also depends on the energy of the events. For a $M_B = -25$ mag source, the deduced rate is $\approx 20 \text{ SN/yr}$.
4. The shape of the events is given by the SN+cSNR light curve represented in fig.1, which depends on the energy ($\epsilon_B \approx 0.5$) and the characteristic time-scale of the pulses (t_{sg}). This last parameter actually controls the shape of the light curve, and remains free. However, its value can be constrained to a narrow band. The values of t_{sg} found to reproduce well isolated peaks in the light curves of NGC 4151 and NGC 5548 are 260–280 days (AT93, AT94), but since high luminosity QSOs may have higher metallicities (Hamann & Ferland 1993), the evolution of their cSNRs could be substantially faster, as cooling rates increase with metallicity.

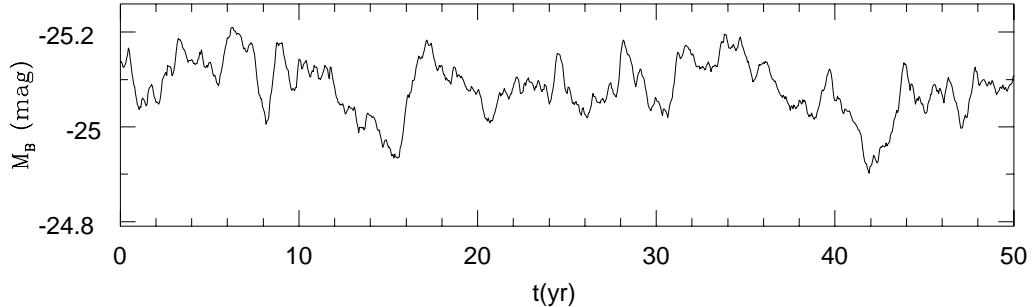


Fig. 2. B -band light curve of a cluster undergoing SN explosions at a rate $\nu_{SN} = 20 \text{ yr}^{-1}$. The time-scale of the cSNRs is $t_{sg} = 280$ days, which gives the highest possible asymmetry.

4.4. Comparison with the data

It should be noted the good agreement between the predicted values derived from the starburst model and the empirically determined values in section 2.2 : $f_{bck} < 0.7$, $1.5 \times 10^{50} \lesssim \epsilon \lesssim 6.3 \times 10^{51} \text{ erg}$, and $1.5 \lesssim \tau \lesssim 3 \text{ yr}$ where the life-time of the pulses and the cooling-time are related by $\tau \approx 5t_{sg}$.

Most importantly, the luminosity–SN rate relationship of eq.1 gives the zero-point of the variability–luminosity relationship. Monte Carlo simulations of stellar clusters undergoing SN explosions show that this scaling matches the zero-point of the variability–luminosity relationship of QSOs once single pass-band data are corrected for wavelength-effects (ACT96). The agreement is good for models with time-scales $85 \lesssim t_{sg} \lesssim 280$ days and objects spanning 7 magnitudes. The analysis of ensemble light curves doesn’t show any clear variations of t_{sg} with redshift, although some evolution is expected and this might be reflected by the goodness of models with different t_{sg} values.

The asymmetry of the cSNR light curves and the apparent time-reversibility of QSO light curves was pointed out as a potential problem by M. Malkan during this conference. To address this issue, in collaboration with S. Cristiani we run some simple tests on the B -band light curves of 180 QSOs monitored for 18 epochs over 10 years (Cristiani et al. 1996). The ensemble skewness of the variations of the sample was measured, finding that within the error bars the number of increases is the same as the number of decreases over the different luminosity variation intervals. The same is true for theoretical light-curves generated using the simple semi-analytical solution of fig.1 (dotted line) once sampling and observational errors are introduced. One should note that even error-free infinitely-sampled light curves built up from the superposition of cSNR units look very symmetric due to the high number of events superposed — see fig.2 for a $M_B = -25$ mag theoretical light curve — much more when sampling (just 20 epochs scattered in 10 years) and observational errors (about 0.1 mag for most samples) are introduced.

For typical QSOs with luminosities between -24 and -27 mag, the SN rate varies between 5 and 100 yr^{-1} and the masses of the postulated coeval stellar clusters vary from 2×10^{10} to $3 \times 10^{11} M_{\odot}$ for a solar neighbourhood IMF (AT94). The mass estimation changes with the IMF and the age of the cluster. The derived masses are well inside the hypothesis of Terlevich & Boyle (1993) that the QSO phenomenon might correspond to the formation of the cores of nowadays normal elliptical galaxies at $z \gtrsim 2$.

For the Seyfert 1 nuclei NGC 4151 and NGC 5548 the SN rates derived from the luminosity are 0.2 and 0.3 yr^{-1} respectively, the energy of the events derived from $W_{H\beta}$ is $\epsilon_B \approx 0.5$ and the time-scale of the pulses can be deduced from isolated pulses of variation like the one in fig.1 to be $t_{sg} \approx 280$ days. Monte Carlo simulations of models with these parameters reproduce in detail the main weak-scale characteristics of the light curves, their rms and power spectra (AT93, AT94).

The low rate of events also explains the temporal disappearance or appearance of broad lines in objects which are traditionally classified as Seyfert 1 or Seyfert 2 and LINERs, respectively. Quiescent stages with undetectable broad lines occur at deep photometric minima. The transitions could be produced in periods of time in which the existing remnants are too old to produce broad lines and the probability of a new explosion which refuels the broad line region is very low. The continuum in these epochs is still blue because the light is dominated by young main sequence stars. A comparison between the probability for this process to happen and recorded occurrences of type transitions shows that all the AGN which have changed types of activity are within the threshold $\overline{M}_B \gtrsim -22.5 \text{ mag}$ (Aretxaga & Terlevich 1994b). For objects of higher luminosity the

probability of a new explosion at any given time would be too high to allow the broad lines to disappear.

Although the optical light curves of radio-quiet AGN follow the predictions of the starburst model, not all AGN follow that pattern. For example, in the historical light curve of the OVV QSO 3C345 (Babadzhanyants et al. 1995) a very similar ‘basic unit of variation’ can also be isolated, but the total luminosity of the source $M_B \approx -26.6$ mag predicts a too high rate of events to account for the 3 mag amplitude variations in B -band. Blazars and OVV QSOs are a minor brand of radio-loud AGN in which other mechanisms should be in play.

5. CONCLUSIONS

The optical variability of radio-quiet AGN is found to be consistent with simple Poissonian processes. A potential basic unit of variation is identified in Seyfert nuclei. The energies and time-scales of this unit are similar to those of nearby SNe and cSNRs. The energies, time-scales and rates of the events empirically found in large databases of QSOs are consistent with those expected from the starburst model of AGN. Two strong predictions are confirmed by these objects: (a) the number of events scales with luminosity, with the zero-point derived from stellar evolution (eq.1) and (b) if the energy per supernova has a universal value, then the equivalent width of $H\beta$ in AGN with broad lines should be constrained to a narrow range of values (eq.2).

ACKNOWLEDGMENTS

It is a pleasure to acknowledge R. Cid Fernandes, S. Cristiani, L. Sodr  and R. Terlevich with whom most of the work presented here has been done, and I. Salamanca for comments on an early draft of this paper. IA’s work is supported by the EEC fellowship ERBCHBICT941023.

REFERENCES

- Alloin D., Pelat D., Phillips M.M., Fosbury R.A.E., Freeman K. 1986, ApJ, 308,23.
Aretxaga I., Terlevich R.J. 1993, ApSS, 206,69 (*AT93*).
Aretxaga I., Terlevich R.J. 1994a, MNRAS, 269,462 (*AT94*).
Aretxaga I., Terlevich R.J. 1994b, in “Violent Star Formation: from 30 Doradus to QSOs” Ed. G. Tenorio-Tagle. CUP, p. 347.
Aretxaga I., Cid Fernandes R., Terlevich R.J. 1996, MNRAS, submitted (*ACT96*).
Babadzhanyants M.K., Belokon E.T., Gamm N.G. 1995, Astr. Rep., 4,447.
Branch D., Falk S.W., McCall M.L., Rybski P., Uomoto A.K., Wills B.J. 1981, ApJ, 244,780.
Cid Fernandes R., Aretxaga I., Terlevich R.J., 1996, MNRAS, in press (*CAT96*).
Cid Fernandes R., Terlevich R.J., Aretxaga I., 1996, MNRAS, submitted.
Cristiani S., Trentini S., La Franca F., Aretxaga I., Andreani P., Vio R. 1996, A&A, 306,395
Dultzin-Hazcyan D., Schuster W.J., Parrao L., Pe a J.H., Peniche R., Benitez E., Costero R. 1992, AJ, 103,1769.
Filippenko A.V. 1989, AJ, 97,726.
Gopal-Krishna, Wiita P.J., Altieri B. 1995, MNRAS, 275,976.
Hamman F., Ferland G. 1993, ApJ, 418,11.
Hook I.M., McMahon R.G., Boyle B.J., Irwin M.J., 1994, MNRAS, 268,305.
Iijima T., Rafanelli P., Bianchini A. 1992, A&A, 265,L25.
Kinney A.L., Bohlin R.C., Blades J.C., York D.G. 1991, ApJS, 75,645.
Korista et al. 1995, ApJS, 97,285.
Osterbrock D.E. 1991, Rep. Prog. Phys., 54,579.
Paltani S., Courvoisier T. 1994, A&A, 291,74.
Pica A.J., Smith A.G. 1983, ApJ, 272,11.
Plewa T. 1995, MNRAS, 275,143.
Rees M. 1984, ARAA, 22,471.
Smith A.G., Nair A.D., Clemens S.D.1991, “Variability of AGN” Eds. H.R. Miller & P.J. Wiita. CUP, p. 52.
Storchi-Bergmann T., Baldwin J.A., Wilson A.S. 1993, ApJ, 419,L11.
Terlevich R.J., Boyle B.J.1993,MNRAS, 262,491
Terlevich R.J., Tenorio-Tagle G., Franco J., Melnick J., 1992, MNRAS, 255,713
Tran H.D., Osterbrock D.E., Martel A. 1992, AJ, 104,2072.
Wagner S., S nchez-Pons F., Quirrebanch A., Witzel A. 1990, A&A, 235, L1.
Wallinder F.H., Kato S., Abramowicz M.A. 1992, A&ARev, 4,79.